CCS Chemistry

COMMUNICATION

Received: June 25, 2021 | Accepted: Aug. 23, 2021 | Published: Sept. 21, 2021

Helical Covalent Polymers with Unidirectional Ion Channels as Single Lithium-Ion Conducting Electrolytes

Yiming Hu[1], Nathan Dunlap[2], Hai Long[3], Hongxuan Chen[1], Lacey J. Wayment[1], Michael Ortiz[1], Yinghua Jin[1], Abdulrahiman Nijamudheen[4], Jose L. Mendoza-Cortes[4], Se-hee Lee[2]* & Wei Zhang[1]*

[1]*Department of Chemistry, University of Colorado Boulder, Boulder, CO 80309,* [2]*Department of Mechanical Engineering, University of Colorado Boulder, Boulder, CO 80309,* [3]*National Renewable Energy Laboratory, Golden, CO 80401,* [4]*Department of Chemical Engineering and Materials Science, Michigan State University, East Lansing, MI 48824*

**Corresponding authors: Sehee.Lee@Colorado.EDU; Wei.Zhang@Colorado.EDU*

Cite this: *CCS Chem.* **2021**, *3*, 2762–2770

Single-ion conducting polymer electrolytes have attracted great attention as safe alternatives to liquid electrolytes in high energy density lithium-ion batteries. Herein, we report the first example of a crystalline anionic helical polymer as a single lithium-ion conducting solid polymer electrolyte (SPE). Single-crystal X-ray analysis shows that the polymer folds into densely packed double helices, with bundles of unidirectional negatively charged channels formed that can facilitate lithium-ion transportation. Such a helical covalent polymer (HCP) exhibits excellent room temperature lithium-ion conductivity (1.2×10^{-3} S·cm^{-1}) in the absence of external lithium salts, a high transference number (0.84), low activation energy (0.14 eV), and a wide electrochemical stability window (0.2–5 V). We found that nonflammable, nonvolatile ionic liquid can serve as a solvating medium and excellent conductivity enhancer (>1000 times increase). These ion-conducting properties are comparable to the best polyethylene oxide-based polymer electrolytes mixed with lithium salts. Finally, we show that the solvated HCP SPE enables the reversible cycling of an all-solid-state cell prepared with a high-voltage NMC 811 cathode. Our study opens up new possibilities for developing next-generation high-performance solid-state electrolytes.

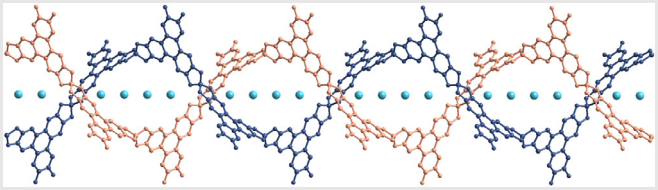

Keywords: **helical covalent polymer, spiroborate, single-ion conducting electrolyte**

Introduction

Lithium-ion batteries power a majority of the world's portable electronics in our daily life, from cell phones to laptops. However, the current flammable liquid electrolytes used in lithium-ion batteries raise potential safety concerns due to problems with overheating and leakage. Solid-state electrolytes overcome most of the safety issues associated with liquid electrolytes. Recently, solid polymer electrolytes (SPEs) composed of lithium salts and a polymer matrix have attracted great attention due to their structural tunability, high mechanical strength, light weight, and flexibility.[1] So far, most of the SPEs are composed of doped Li salts in a neutral polymer matrix [e.g., polyethylene oxide (PEO)], in which both cations and anions migrate and contribute to the measured conductivity.[2] In such dual-ion conducting systems, the Li-ion transference number (Li-ion conductivity/overall conductivity × 100%) is generally below 50%, limiting charge and discharge rates and the power output of the

DOI: 10.31635/ccschem.021.202101257
Citation: *CCS Chem.* **2021**, 3, 2762–2770
Citation denotes calendar and volume year of first online publication.
Issue Assignment: Volume 3 (2021), Issue 12

battery.[3-5] One way to immobilize anions and only allow cation mobility is to covalently attach anions to the polymer backbones. Single-ion conducting polymer electrolytes (SICPEs) with immobilized anions can provide a high Li-ion transference number (>0.7) and reduce the buildup of ion concentration gradients and lithium dendrites growth, thus greatly enhancing energy efficiency and cell lifetime.[6-9]

SICPEs have mostly been prepared by covalently attaching anionic side groups to the backbone of polymers.[10] Most SICPEs are thus amorphous, and lithium-ion diffusion and migration are assisted by the segmental motion of the polymer matrix at a temperature above T_g. Although the presence of channels in crystalline domains of some polymer electrolytes (e.g., PEO_6:$LiXF_6$) has been reported to facilitate lithium-ion transport and improve the ion conductivity,[11,12] there have been very few examples of crystalline SICPEs, mostly due to the synthetic challenge of obtaining crystalline polymer materials.[13-16]

Herein, we report the first example of a crystalline linear covalent polymer electrolyte as an efficient SICPE. Similar to PEO-based electrolytes, the linear polymer contains lithium coordinating centers along the backbone structure. However, unlike PEO, the polymer folds into double helices, forming densely packed negatively charged columnar channels, which can efficiently transport lithium cations. Such helical covalent polymer (**HCP**) exhibits excellent room temperature lithium-ion conductivity of 1.2×10^{-3} S·cm^{-1}, a high Li-ion transference value (0.84), low activation energy (0.14 eV atom^{-1}), and a wide electrochemical stability window (0.2–5 V). Importantly, it shows a good chemical compatibility with lithium metal and ultimately enabled the reversible cycling of an all-solid-state Li-ion cell prepared with a high-voltage NMC 811 cathode [NMC = Lithium Nickel Manganese Cobalt Oxide ($LiNi_{0.8}Co_{0.1}Mn_{0.1}O_2$)]. The additional advantages of such **HCP**-based solid electrolytes include light weight, high stability, and well-defined pore structures. Our study, for the first time, reveals the formation of lithium-ion channels in a crystalline linear polymer, and provides an interesting direction for the future design of highly efficient SICPEs.

Results and Discussion

Spiroborates are unique anions that can be reversibly formed through the condensation of diols and boronic acids yet are resistant to hydrolysis and stable in water, methanol, and even alkaline solutions.[17,18] Owing to their reversible nature, spiroborate linkages have been applied in the dynamic assembly of multianionic discrete structures, such as macrocycles and cages,[17,19-21] which have shown interesting applications as electrolytes,[22] sensors,[23,24] catalysts,[25] and hosts of neutral molecules or ions.[26-28] Previously, we developed an efficient method to prepare anionic alkyl borate-linked ionic covalent organic frameworks (ICOFs) with lithium-ion conducting properties (Scheme 1).[16] It has been reported that the charge delocalization of borate anions can improve the electrochemical performance and stabilities.[29] We used Gaussian 16[30] to perform density functional theory (DFT) geometry optimization for the two structures shown in Scheme 1 with the B3LYP method,[31] the 6-311++G(2d,p) basis set, and the polarizable continuum model (PCM) solvation model[32] of acetonitrile solvents. The Li^+ binding energy can be obtained by comparing the energies between the Li^+-complex structure and the individual complex with Li^+. The calculated binding energies for the "previous work" and "this work" structures are 12.1 and 6.2 kcal/mol, respectively, validating our assumption that better conjugation would weaken the interaction between BO_4^- and Li^+. Therefore, in this work, we selected 2,3,6,7,10,11-hexahydroxytriphenylene (HHTP) with a large conjugated aromatic system as a multi-diol monomer (Scheme 1). We envisioned that if the negative charges of borate anions are delocalized by surrounding conjugate systems, the formation of tight ion pairs would be suppressed, which would facilitate lithium-ion migration and enhance the ion conductivity. The condensation HHTP with $B(OMe)_3$ in the presence of LiOH provided the crystalline **HCP** (Figures 1a and 1b). The structure, conformation, and the packing mode of the **HCP** were unambiguously determined by single-crystal X-ray diffraction with discrepancy factor R of 10.71%.[33]

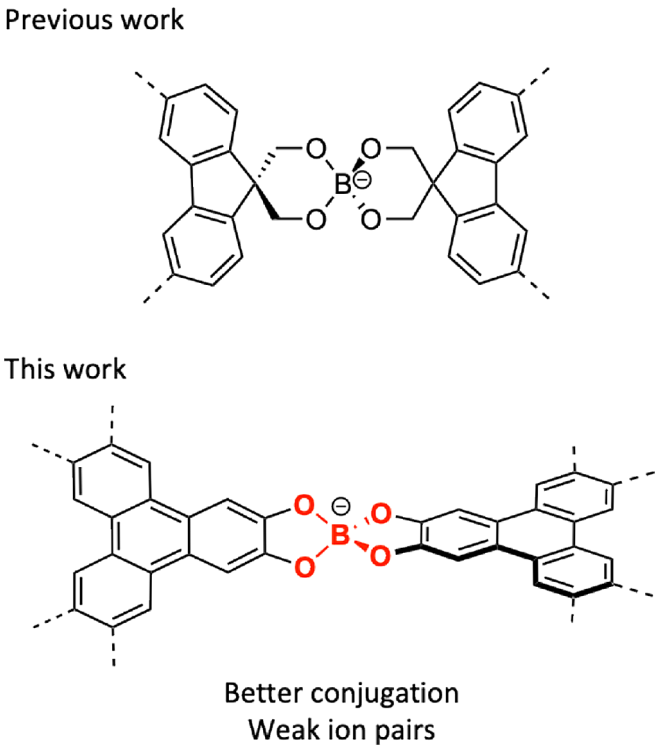

Scheme 1 | *Alkyl spiroborate and aryl spiroborate structures.*

DOI: 10.31635/ccschem.021.202101257
Citation: *CCS Chem.* **2021**, 3, 2762–2770
Citation denotes calendar and volume year of first online publication.
Issue Assignment: Volume 3 (2021), Issue 12

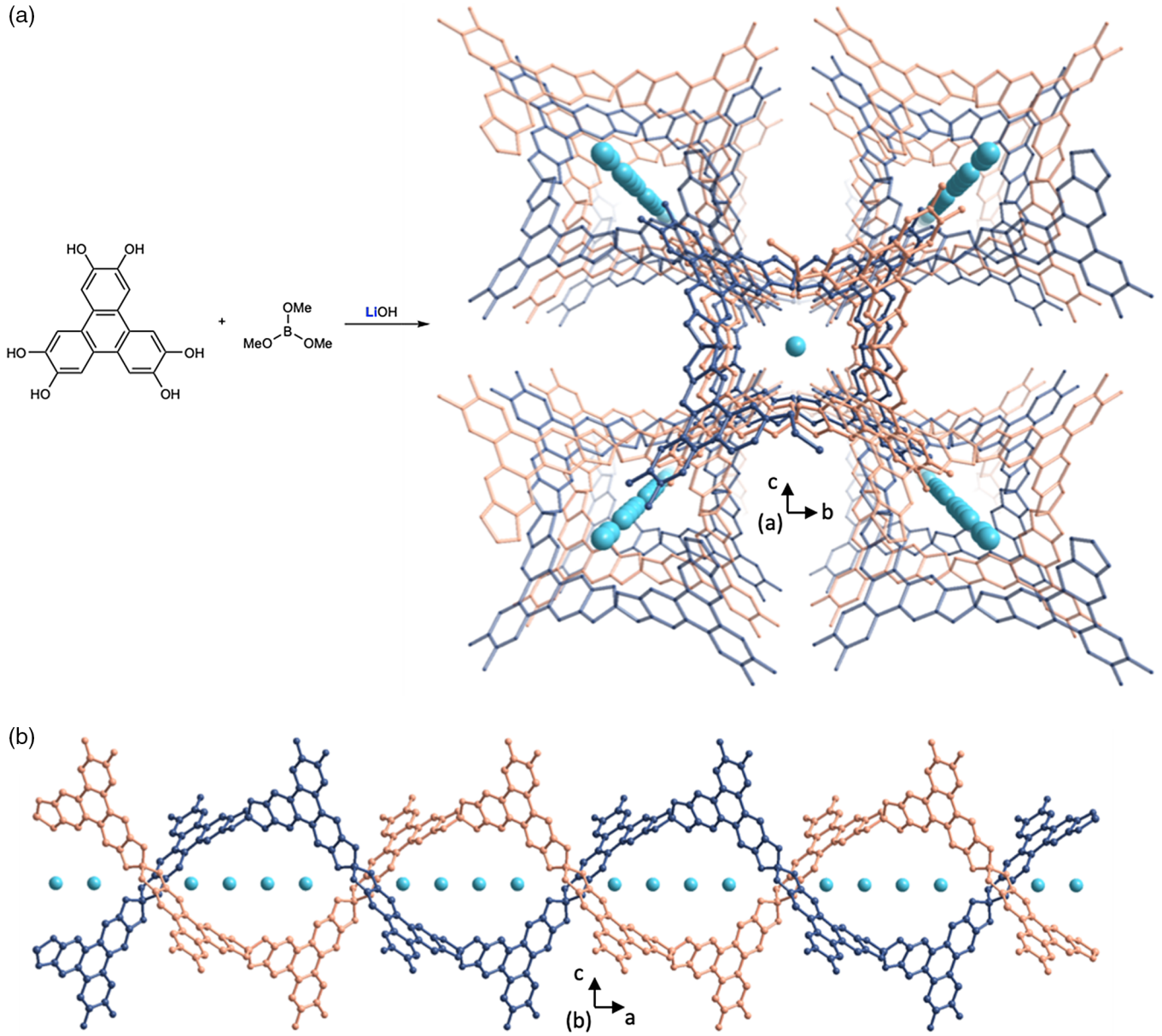

Figure 1 | *Synthesis of **HCP** and its crystal structure: Top view (a) and side view (b) of the internal cavity of the **HCP**. Two chains are colored in green and brown, and the Li ion is colored in blue.*

The single-crystal X-ray structure clearly shows that the linear polymer folds into a double helical conformation of tubular channels. Each wall of the square-shaped channel consists of linearly aligned spiroborate anions along the helical axis at every 15.2 Å, providing negatively charged channels. We found that the lithium cations are located at the center of the rigid columnar channels. It is interesting to note that only two pairs of diols of each HHTP reacted, and the unreacted diol formed multiple hydrogen bonds with spiroborate anions of the neighboring helical strand, thus forming a densely packed array of charged columnar channels. Although double helices of the **HCP** are packed through hydrogen bonding interactions, the crystal showed excellent stability in various organic solvents and water. The crude **HCP** was washed in open air with a large amount of benchtop solvents, such as methylene chloride, acetone, and tetrahydrofuran (THF). The product can also survive heated conditions for a long time (Soxhlet extraction with THF for 2 days). Unlike polymers linked by boronic esters that are very prone to hydrolysis, the **HCP** has high stability in water, showing similar powder X-ray diffraction (PXRD) measurements even after soaking in water for 48 h.[33] **HCP** also exhibits high thermal stability, showing <5% weight loss at 300 °C according to the thermogravimetric analysis (TGA) results (Supporting Information Figure S1). The PXRD patterns of as-synthesized bulk **HCP** materials

DOI: 10.31635/ccschem.021.202101257
Citation: *CCS Chem.* **2021**, 3, 2762–2770
Citation denotes calendar and volume year of first online publication.
Issue Assignment: Volume 3 (2021), Issue 12

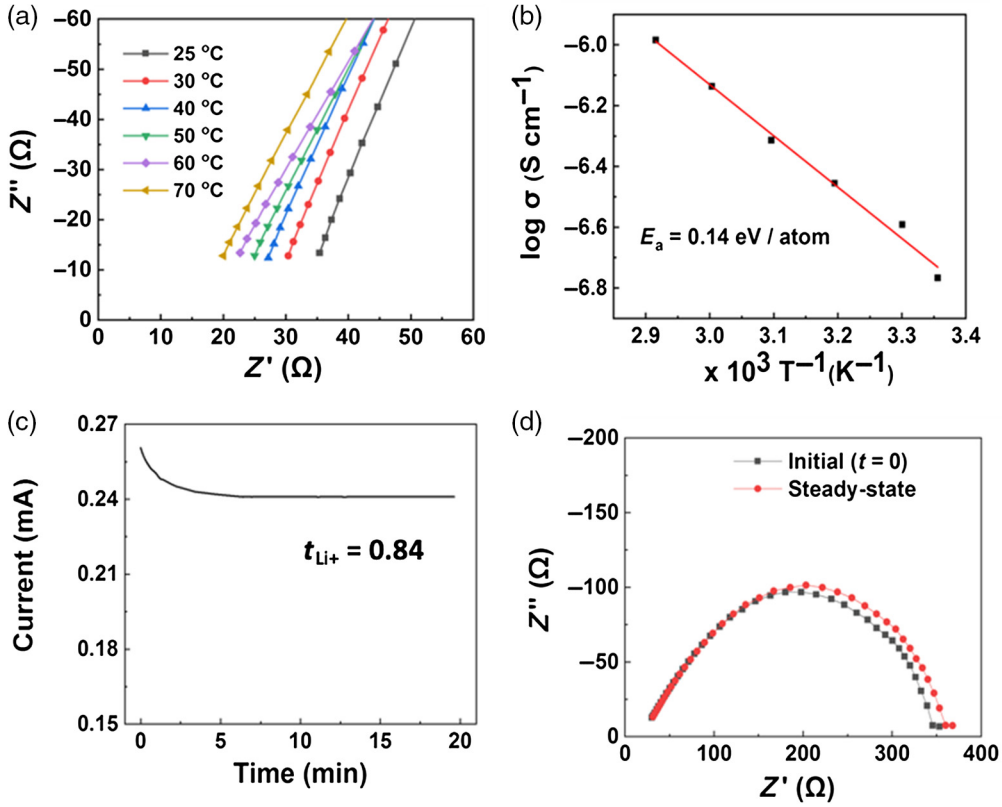

Figure 2 | *Electrochemical measurements of **HCP** pellets solvated with $PYR_{13}FSI$ IL: (a) Nyquist plots of EIS measurements over a range of temperatures. (b) Arrhenius plot of ionic conductivity as a function of temperature. (c) Lithium transference number as calculated using BVE technique. (d) Impedance before and after lithium transference number measurement.*

match the simulation very well based on the single-crystal structure (Supporting Information Figure S2), indicating that the bulk sample has the same crystalline structure as the single crystal. The scanning electron microscopy (SEM) image of the bulk **HCP** shows cuboid-shaped crystals similar to the shape of the crystals used for single-crystal X-ray analysis (Supporting Information Figure S3).

The negatively charged one-dimensional (1D) channels, their dense packing, and the chemical and thermal stability suggest that the **HCP** would excel as a lightweight stable single-ion conducting solid-state electrolyte. The lithium-ion conductivity of the **HCP** was thus examined. Prior to testing, the **HCP** was vacuum-dried overnight at 120 °C. Electrochemical analysis was performed on dense pellets of the **HCP** pressed within custom 13 mm diameter all-solid-state cell dies (Supporting Information Scheme S1). While the dry **HCP** is a modest Li-ion conductor, we found that its conductivity increased by several orders of magnitude upon solvation by $PYR_{13}FSI$ ionic liquid (IL) composed of bis(fluorosulfonyl)imide (FSI^-) anions and *N*-propyl-*N*-methylpyrrolidinium (PYR_{13}^+) cations. Previously, it has been reported that lithium salt/$PYR_{13}FSI$ mixture is capable of forming stable solid electrolyte interfaces (SEIs) with a variety of electrode materials and can be used as a liquid electrolyte in Li-ion batteries.[34] However, it has never been used as a solvating medium. Before testing the conductivity of the **HCP**, one drop of $PYR_{13}FSI$ was deposited onto the dense **HCP** pellet and allowed to soak for approximately 1 h. Electrochemical impedance spectroscopy (EIS) was used to measure the ionic conductivity of the solvated **HCP**. Nyquist plots in Figure 2a show a steep spike characteristic of the low frequency capacitive nature of conformal electrolyte interfaces with Li-ion blocking electrodes. A high room-temperature conductivity of 1.2×10^{-3} S·cm^{-1} was measured, which is comparable to the best PEO-based electrolytes reported[35] and is nearly an order of magnitude higher than the conductivity reported for similar single-ion polymer electrolyte materials.[36] It should be noted that the ionic conductivity of **HCP** is significantly higher than that of the ICOF (3.05×10^{-5} S cm^{-1}) consisting of alkyl spiroborates,[16] supporting the notion that Li^+ and aryl-spiroborate anion interactions are weakened due to the charge delocalization in the conjugated aromatic system, leading to enhanced lithium-ion mobility and higher ionic

DOI: 10.31635/ccschem.021.202101257
Citation: *CCS Chem.* **2021**, 3, 2762–2770
Citation denotes calendar and volume year of first online publication.
Issue Assignment: Volume 3 (2021), Issue 12

conductivity. Due to such high conductivity of the solvated **HCP**, the high frequency semicircles, typical of Nyquist plots, could not be captured under the temperature and frequency range of this experiment. Therefore, contributions due to ohmic, grain boundary, and bulk resistance could not be differentiated. However, all are included in determining the overall conductivity of **HCP**.

Previously, covalent organic framework (COF) microcrystalline powders have been mixed with large mass fractions (>30%) of polymeric binders to prepare free-standing drop cast films.[37] While these composites are mechanically robust, the uneven distribution of COF powders negatively impacts the movement of Li ions through films. Thick coatings of resistive polymer binders act like roadblocks of diffusing Li ions, restricting the overall conductivity of solid electrolyte films. By pressing the dense binder-free crystals of the **HCP** sample, we can better ensure that the conduction pathways through the 1D columnar channels, intrinsic to this unique double helical polymer, remain open for the unimpeded conduction of Li ions. When polyvinylidene fluoride (PVDF) was used as the binder, the **HCP**/PVDF composite only showed 10% conductivity of that of the binder-free **HCP** electrolyte under the identical conditions (Supporting Information Figure S7). To the best of our knowledge, this is the first report that demonstrates the single-ion conductivity enhancement of a pure linear polymer by solvating with an IL. It should be noted that the $PYR_{13}FSI$ used in this study contains no dissolved external Li salts, and therefore it is not expected to contribute directly to the measured Li-ion conductivity of the **HCP** crystals. Instead, its high dielectric constant and large anions promote the dissociation of loosely bound Li ions from the anionic **HCP** backbone, allowing them to quickly transport through the bundles of the 1D columnar channels packed along the same direction. It was found that a single drop of IL, constituting approximately 20 wt % of the pellets mass, was enough to achieve maximum conductivity from **HCP**. This is much lower than the mass loading of organic solvents reported in studies of similar single-ion polymer conductors and more heavily researched polymer electrolytes such as PEO, which commonly call for solvent loadings exceeding 90 wt %.[3,4,35,38] Large additions of organic additives reduce the structural integrity of polymer electrolytes and lead to electrochemical, thermal, and chemical instabilities. By solvating with just one drop of IL, the pressed **HCP** crystals retain their crystallinity (Supporting Information Figure S2) and remain mechanically robust, as shown in Supporting Information Figure S5. The inflammability, low volatility, negligible vapor pressure, and wide window of electrochemical, thermal, and chemical stability also represent significant advantages of $PYR_{13}FSI$ as a solvating medium in solid electrolytes. To further demonstrate the effect of an IL on the conductivity of a solid electrolyte, we also tested the propylene carbonate (PC) and $PYR_{14}TFSI$ as plasticizers. The Nyquist plots of impedance test results showed that when PC was added, the **HCP** electrolyte showed a conductivity of 5.6×10^{-5} S cm^{-1}, whereas when $PYR_{14}TFSI$ was added, a much higher conductivity of 1.0×10^{-3} S cm^{-1} was obtained, which is similar to that observed for the $PYR_{13}FSI$-soaked **HCP** electrolyte (Supporting Information Figures S6 and S8). These results further support the boosting effect of an IL on electrolyte conductivity, and such effect is likely general.

The Arrhenius plot in Figure 2b shows that the **HCP** displays a linear (Arrhenius) activation energy relationship, which indicates that the conduction of Li ions is decoupled from the negatively charged **HCP** skeleton. This is an uncommon characteristic in organic solid electrolytes that can be attributed to the rigid and uniquely ordered structure of **HCP**. Most solid organic and liquid electrolytes, $PYR_{13}FSI$ included, display nonlinear activation energies at elevated temperatures, a phenomenon that can be closely approximated by the well-known Vogel–Tammann–Fulcher (VTF) equation. [5,39] The Arrhenius nature of **HCP** suggests that its conductivity is attributed to a mechanism similar to the hopping of Li ions between lattice sites in an inorganic crystalline solid electrolyte rather than simply dissolving and diffusing through the solvating IL. The remarkably low activation energy of 0.14 eV atom^{-1} determined for **HCP** is similar to the best-performing COF materials reported previously as well as some of the best inorganic solid electrolytes.[40]

In conventional electrolytes, Li salts are dissolved into a polar solvent, allowing for the diffusion of both Li^+ cations and mobile anions. This results in poor average Li^+ transference numbers leading to the buildup of concentration gradients that cause polarization in the electrolyte. **HCP** has 1D columnar channels with negatively charged groups permanently immobilized on the wall; thus migration of anions is prohibited. The average Li^+ transference number of the **HCP** based electrolyte was determined to be 0.84 using the Bruce–Vincent–Evans (BVE) method (Figures 2c and 2d). Therefore, the average Li^+ transference number close to unity represents significant improvement compared to electrolytes based on lithium salts dissolved in ILs or solid polymers such as PEO, which typically range from 0.2 to 0.5.[3-5] The large Li^+ transference number represents further evidence that the IL added to the **HCP** is not the primary source of Li-ion conduction. Rather, the IL solvates the **HCP**, reducing the Li^+ binding energy, loosening them up for faster conduction through the **HCP**'s atomically precise 1D channels.

The cyclic voltammogram (Figure 3a) of the **HCP** displays a wide window of electrochemical stability. No significant current flow corresponding to electrolyte decomposition was observed up to 5 V. Only cathodic

DOI: 10.31635/ccschem.021.202101257
Citation: *CCS Chem.* **2021**, 3, 2762–2770
Citation denotes calendar and volume year of first online publication.
Issue Assignment: Volume 3 (2021), Issue 12

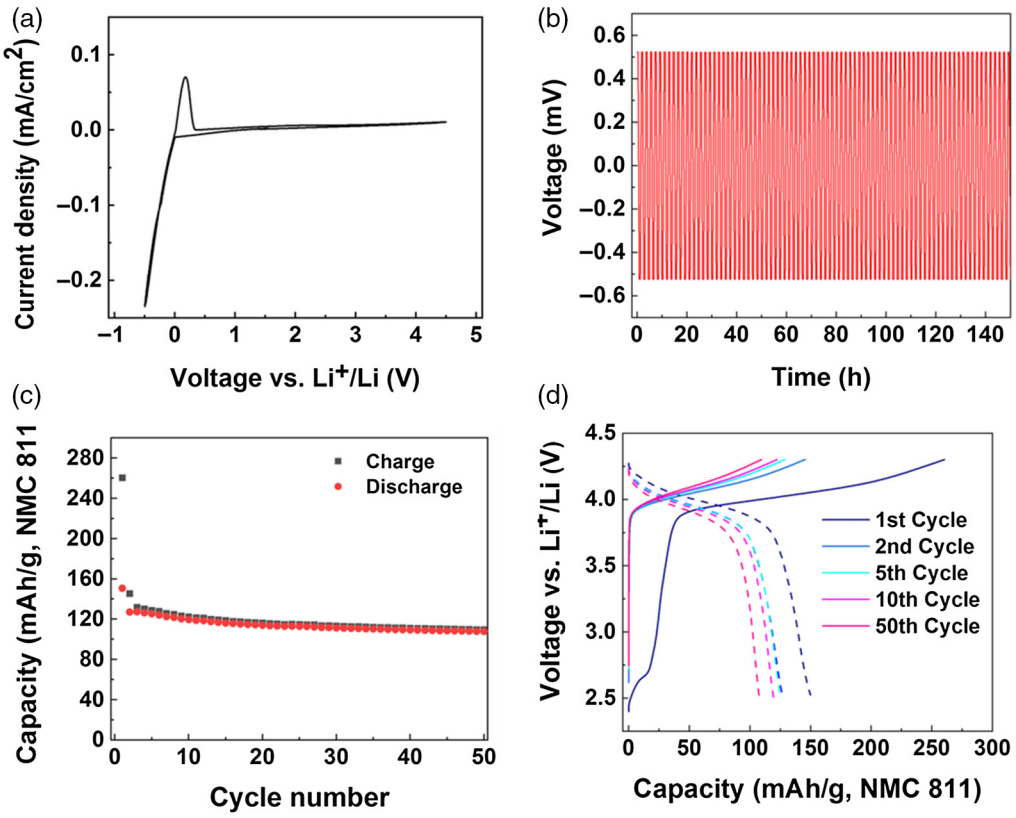

Figure 3 | *(a) Cyclic voltammogram of the Ti/**HCP**/Li cell. (b) Cycling stability of a symmetric Li/**HCP**/Li cell cycled at room temperature with a current density of 0.1 mA cm^{-2}. (c) Cycling data for LiIn/**HCP**/NMC 811 battery. (d) Corresponding voltage profile of LiIn/**HCP**/NMC (solid line: charge; dash line: discharge).*

and anodic currents corresponding to lithium deposition ($Li^+ + e^- \rightarrow Li$) and stripping ($Li \rightarrow Li^+ + e^-$) were observed near 0 V versus Li, indicating the capability of Li-ion conduction through the electrolyte. The surface morphology of Li metal was also investigated by ex situ SEM (Supporting Information Figure S4). A smooth Li metal surface was observed after 10 cycles of stripping and plating, indicating the compatibility of organic electrolyte and Li metal and its ability to enable uniform, dendrite-free plating. Linear sweep voltammograms of the remaining **HCP** (Supporting Information Figure S9) show that they are fairly stable up to ~5 V. The sloping profile between 0.2 and 6 V is characteristic for a dense pellet of low resistance solid electrolyte powders. Above 5 V, a current spike is observed, which can be attributed to the breakdown of $PYR_{13}FSI$ with lithium, as previously reported.[41] This demonstrates the potential compatibility of **HCP** with high-voltage, high-power cathode materials.

The electrochemical stability and large effective conductivity allowed a Li/**HCP**/Li symmetric cell to achieve >150 galvanostatic deposition/stripping for 150 h at room temperature (Figure 3b). The stability of the cell's voltage profile further confirms the **HCP**'s compatibility with metallic lithium. The ionic conductivity estimated from direct current (DC) polarization is on the same order of magnitude as that obtained from room-temperature EIS measurements. These results suggest that the organic electrolyte material could prove useful in the next generation of Li-metal batteries, which promises to provide energy densities beyond the theoretical maximum achievable by todays Li-ion cells.

The **HCP** electrolyte's wide window of electrochemical stability enabled the reversible cycling of a high voltage NMC 811 composite cathode (Figure 3c). The battery was assembled in a solid-state fashion and performed at 60 °C with a cycling rate of 0.1 C for 50 cycles. Upon its first charge, this cell achieved an active material specific capacity >260 mAh/g, significantly exceeding the theoretical limit of NMC 811 (200 mAh/g). The cell's voltage profile (Figure 3d) shows that the extra capacity originates from a low voltage (~2.6 V) charging event not usually associated with layered NMC materials. This unexpected charge capacity indicates that upon assembly, the cell was momentarily short-circuited, resulting in self-discharge and overlithiation of the cathode's active materials. This overlithiated plateau accounts for ~50 mAh/g (NMC 811) of extra capacity in our cell, which is well within the range of stable overlithiation outlined in reported literature.[42,43] Upon discharging, only 57.8% of the large initial charge

DOI: 10.31635/ccschem.021.202101257
Citation: *CCS Chem.* **2021**, 3, 2762–2770
Citation denotes calendar and volume year of first online publication.
Issue Assignment: Volume 3 (2021), Issue 12

capacity was reversible, but if the low voltage (~2.6 V) irreversible capacity were to be excluded, the Coulombic efficiency would approach 75%. With continued cycling, the cell's capacity quickly stabilized to ~120 mAh/g with Coulombic efficiencies >98% after only four cycles. These preliminary results indicate that the high conductivity and stability of **HCP** can in fact enable the reversible cycling of modern nickel-rich cathode materials, although further work is needed to optimize the performance of this particular system.

Finally, it was in fact found that the facile Li-ion conductivity of the **HCP** electrolyte enabled the prolonged reversible cycling of a high-voltage all-solid-state cell. Despite some irreversibility in its initial charge capacity, the all-solid-state cell achieves a remarkably stable specific capacity of ~120 mAh/g over 50 cycles. Further optimization of the cell's construction and composition as well as widening of the cell's voltage window ~4.5 V will certainly lead to improved first-cycle Coulombic efficiency and cathode capacity, respectively. Nonetheless, these present results clearly demonstrate the **HCP** electrolyte's ability to enable the reversible cycling of a high-voltage all-solid-state cell.

Conclusion

We have developed a highly stable and ordered crystalline **HCP**, consisting of negatively charged 1D columnar channels with mobile Li^+ counter cations, as a single-ion conducing polymer electrolyte. For the first time, the aryl-spiroborate linkages are used to introduce immobilized negative charges, which form loose ion pairs and assist the migration of lithium cations. Solvation with a small quantity of IL allows the **HCP** to achieve high Li-conductivity (room temperature conductivity of 1.2×10^{-3} S cm^{-1}) with a high lithium-ion transference number (0.84), while remaining mechanically robust and electrochemically stable up to 5 V versus Li^+/Li. These superior properties of the **HCP** as solid-state electrolytes are mainly attributed to the highly ordered and well-defined pathway of mobile lithium ions through the rigid 1D channels of **HCP** and the formation of loose aryl-spiroborate/lithium ion pairs. This is also the first report demonstrating the use of highly stable $PYR_{13}FSI$ IL to enhance the conductivity of a single-ion conducting polymer. The outstanding stability of the combined organic electrolyte–IL with lithium metal is demonstrated through extended, plating/stripping of a Li/**HCP**/Li symmetric cell, accompanied with ex-situ SEM analysis of a cycled Li-metal electrode. Finally, the practical Li-ion conductivity and high voltage stability of the **HCP** electrolyte is conclusively demonstrated through the reversible cycling of a modern Ni-rich NMC 811 cathode in an all-solid-state cell. Our study opens up new possibilities for designing and fabricating lightweight, stable, and highly ion-conductive solid-state electrolytes for future lithium-metal battery applications.

Supporting Information

Supporting Information is available and includes experimental methods, characterization data (TGA, PXRD, SEM), additional figures, and EIS results.

Conflict of Interest

There is no conflict of interest to report.

Funding Information

This work was supported by the University of Colorado Boulder.

Acknowledgments

The authors thank D. Gin for the assistance with the PXRD experiments.

References

1. Hu, Y.; Wayment, L. J.; Haslam, C.; Yang, X.; Lee, S.-H.; Jin, Y.; Zhang, W. Covalent Organic Framework Based Lithium-Ion Battery: Fundamental, Design and Characterization. *EnergyChem* **2021**, *3*, 100048.
2. Agrawal, R. C.; Pandey, G. P. Solid Polymer Electrolytes: Materials Designing and All-Solid-State Battery Applications: An Overview. *J. Phys. D Appl. Phys* **2008**, *41*, 223001.
3. Tiyapiboonchaiya, C.; Pringle, J. M.; MacFarlane, D. R.; Forsyth, M.; Sun, J. Z. Polyelectrolyte-in-Ionic-Liquid Electrolytes. *Macromol. Chem. Phys.* **2003**, *204*, 2147–2154.
4. Sun, J.; MacFarlane, D. R.; Forsyth, M. Lithium Polyelectrolyte-Ionic Liquid Systems. *Solid State Ion.* **2002**, *147*, 333–339.
5. Kunze, M.; Jeong, S.; Appetecchi, G. B.; Schonhoff, M.; Winter, M.; Passerini, S. Mixtures of Ionic Liquids for Low Temperature Electrolytes. *Electrochim. Acta* **2012**, *82*, 69–74.
6. Manthiram, A.; Yu, X. W.; Wang, S. F. Lithium Battery Chemistries Enabled by Solid-State Electrolytes. *Nat. Rev. Mater.* **2017**, *2*, 16103.
7. Wiers, B. M.; Foo, M. L.; Balsara, N. P.; Long, J. R. A Solid Lithium Electrolyte via Addition of Lithium Isopropoxide to a Metal-Organic Framework with Open Metal Sites. *J. Am. Chem. Soc.* **2011**, *133*, 14522–14525.
8. Van Humbeck, J. F.; Aubrey, M. L.; Alsbaiee, A.; Ameloot, R.; Coates, G. W.; Dichtel, W. R.; Long, J. R. Tetraarylborate Polymer Networks as Single-Ion Conducting Solid Electrolytes. *Chem. Sci.* **2015**, *6*, 5499–5505.
9. Zhang, H.; Li, C. M.; Piszcz, M.; Coya, E.; Rojo, T.; Rodriguez-Martinez, L. M.; Armand, M.; Zhou, Z. B. Single Lithium-Ion Conducting Solid Polymer Electrolytes: Advances and Perspectives. *Chem. Soc. Rev.* **2017**, *46*, 797–815.
10. Zhu, J. D.; Zhang, Z.; Zhao, S.; Westover, A. S.; Belharouak, I.; Cao, P. F. Single-Ion Conducting Polymer

DOI: 10.31635/ccschem.021.202101257
Citation: *CCS Chem.* **2021**, 3, 2762–2770
Citation denotes calendar and volume year of first online publication.
Issue Assignment: Volume 3 (2021), Issue 12

Electrolytes for Solid-State Lithium-Metal Batteries: Design, Performance, and Challenges. *Adv. Energy Mater.* **2021**, *11*, 2003836.
11. Gadjourova, Z.; Andreev, Y. G.; Tunstall, D. P.; Bruce, P. G. Ionic Conductivity in Crystalline Polymer Electrolytes. *Nature* **2001**, *412*, 520–523.
12. Stoeva, Z.; Martin-Litas, I.; Staunton, E.; Andreev, Y. G.; Bruce, P. G. Ionic Conductivity in the Crystalline Polymer Electrolytes PEO_6: $LiXF_6$, X = P, As, Sb. *J. Am. Chem. Soc.* **2003**, *125*, 4619–4626.
13. Jeong, K.; Park, S.; Jung, G. Y.; Kim, S. H.; Lee, Y. H.; Kwak, S. K.; Lee, S. Y. Solvent-Free, Single Lithium-Ion Conducting Covalent Organic Frameworks. *J. Am. Chem. Soc.* **2019**, *141*, 5880–5885.
14. Zhang, Y. Y.; Duan, J. Y.; Ma, D.; Li, P. F.; Li, S. W.; Li, H. W.; Zhou, J. W.; Ma, X. J.; Feng, X.; Wang, B. Three-Dimensional Anionic Cyclodextrin-Based Covalent Organic Frameworks. *Angew. Chem. Int. Ed.* **2017**, *56*, 16313–16317.
15. Hu, Y.; Dunlap, N.; Wan, S.; Lu, S.; Huang, S.; Sellinger, I.; Ortiz, M.; Jin, Y.; Lee, S.-H.; Zhang, W. Crystalline Lithium Imidazolate Covalent Organic Frameworks with High Li-Ion Conductivity. *J. Am. Chem. Soc.* **2019**, *141*, 7518–7525.
16. Du, Y.; Yang, H.; Whiteley, J. M.; Wan, S.; Jin, Y.; Lee, S.-H.; Zhang, W. Ionic Covalent Organic Frameworks with Spiroborate Linkage. *Angew. Chem. Int. Ed.* **2016**, *55*, 1737–1741.
17. Abrahams, B. F.; Price, D. J.; Robson, R. Tetraanionic Organoborate Squares Glued Together by Cations to Generate Nanotubular Stacks. *Angew. Chem. Int. Ed.* **2006**, *45*, 806–810.
18. Brown, H. C.; Rangaishenvi, M. V. Organoboranes. 51. Convenient Procedures for the Recovery of Pinanediol in Asymmetric-Synthesis via One-Carbon Homologation of Boronic Esters. *J. Organomet. Chem.* **1988**, *358*, 15–30.
19. Loewer, Y.; Weiss, C.; Biju, A. T.; Frohlich, R.; Glorius, F. Synthesis and Application of a Chiral Diborate. *J. Org. Chem.* **2011**, *76*, 2324–2327.
20. Danjo, H.; Hirata, K.; Yoshigai, S.; Azumaya, I.; Yamaguchi, K. Back to Back Twin Bowls of D-3-Symmetric Tris(spiroborate)s for Supramolecular Chain Structures. *J. Am. Chem. Soc.* **2009**, *131*, 1638–1693.
21. Danjo, H.; Mitani, N.; Muraki, Y.; Kawahata, M.; Azumaya, I.; Yamaguchi, K.; Miyazawa, T. Tris(spiroborate)-Type Anionic Nanocycles. *Chem. Asian J.* **2012**, *7*, 1529–1532.
22. Danjo, H.; Hashimoto, Y.; Kidena, Y.; Nogamine, A.; Katagiri, K.; Kawahata, M.; Miyazawa, T.; Yamaguchi, K. Nestable Tetrakis(spiroborate) Nanocycles. *Org. Lett.* **2015**, *17*, 2154–2157.
23. Moriya, M.; Kato, D.; Sakamoto, W.; Yogo, T. Plastic Crystalline Lithium Salt with Solid-State Ionic Conductivity and High Lithium Transport Number. *Chem. Commun.* **2011**, *47*, 6311–6313.
24. Kameta, N.; Hiratani, K. Synthesis of Supramolecular Boron Complex with Anthryl Groups Exhibiting Specific Optical Response for Chloride Ion. *Tetrahedron Lett.* **2006**, *47*, 4947–4950.
25. Kameta, N.; Hiratani, K. Phosphate Anion-Selective Recognition by Boron Complex Having Plural Hydrogen Bonding Sites. *Chem. Commun.* **2005**, *41*, 725–727.
26. Carter, C.; Fletcher, S.; Nelson, A. Towards Phase-Transfer Catalysts with a Chiral Anion: Inducing Asymmetry in the Reactions of Cations. *Tetrahedron Asymmetry* **2003**, *14*, 1995–2004.
27. Danjo, H.; Hirata, K.; Noda, M.; Uchiyama, S.; Fukui, K.; Kawahata, M.; Azumaya, I.; Yamaguchi, K.; Miyazawa, T. Assembly Modulation by Adjusting Countercharges of Heterobimetallic Supramolecular Polymers Composed of Tris(spiroborate) Twin Bowls. *J. Am. Chem. Soc.* **2010**, *132*, 15556–15558.
28. Danjo, H.; Nakagawa, T.; Katagiri, K.; Kawahata, M.; Yoshigai, S.; Miyazawa, T.; Yamaguchi, K. Formation of Lanthanide(III)-Containing Metallosupramolecular Arrays Induced by Tris(spiroborate) Twin Bowl. *Cryst. Growth Des.* **2015**, *15*, 384–389.
29. Barthel, J.; Buestrich, R.; Gores, H. J.; Schmidt, M.; Wuhr, M. A New Class of Electrochemically and Thermally Stable Lithium Salts for Lithium Battery Electrolytes. 4. Investigations of the Electrochemical Oxidation of Lithium Organoborates. *J. Electrochem. Soc.* **1997**, *144*, 3866–3870.
30. Frisch, M. J.; Trucks, G. W.; Schlegel, H. B.; Scuseria, G. E.; Robb, M. A.; Cheeseman, J. R.; Scalmani, G.; Barone, V.; Petersson, G. A.; Nakatsuji, H.; Li, X.; Caricato, M.; Marenich, A. V.; Bloino, J.; Janesko, B. G.; Gomperts, R.; Mennucci, B.; Hratchian, H. P.; Ortiz, J. V.; Izmaylov, A. F.; Sonnenberg, J. L.; Williams, D.; Ding, F.; Lipparini, F.; Egidi, F.; Goings, J.; Peng, B.; Petrone, A.; Henderson, T.; Ranasinghe, D.; Zakrzewski, V. G.; Gao, J.; Rega, N.; Zheng, G.; Liang, W.; Hada, M.; Ehara, M.; Toyota, K.; Fukuda, R.; Hasegawa, J.; Ishida, M.; Nakajima, T.; Honda, Y.; Kitao, O.; Nakai, H.; Vreven, T.; Throssell, K.; Montgomery, Jr., J. A.; Peralta, J. E.; Ogliaro, F.; Bearpark, M. J.; Heyd, J. J.; Brothers, E. N.; Kudin, K. N.; Staroverov, V. N.; Keith, T. A.; Kobayashi, R.; Normand, J.; Raghavachari, K.; Rendell, A. P.; Burant, J. C.; Iyengar, S. S.; Tomasi, J.; Cossi, M.; Millam, J. M.; Klene, M.; Adamo, C.; Cammi, R.; Ochterski, J. W.; Martin, R. L.; Morokuma, K.; Farkas, O.; Foresman, J. B.; Fox, D. J. *Gaussian 16 Revision C.01*; Gaussian, Inc.: Wallingford, CT, **2016**.
31. Stephens, P. J.; Devlin, F. J.; Chabalowski, C. F.; Frisch, M. J. Ab Initio Calculation of Vibrational Absorption and Circular Dichroism Spectra Using Density Functional Force Fields. *J. Phys. Chem.* **1994**, *98*, 11623–11627.
32. Tomasi, J.; Mennucci, B.; Cammi, R. Quantum Mechanical Continuum Solvation Models. *Chem. Rev.* **2005**, *105*, 2999–3094.
33. Hu, Y.; Teat, S. J.; Gong, W.; Zhou, Z.; Jin, Y.; Chen, H.; Wu, J.; Cui, Y.; Jiang, T.; Cheng, X.; Zhang, W. Single Crystals of Mechanically Entwined Helical Covalent Polymers. *Nat. Chem.* **2021**, *13*, 660–665.
34. Moreno, M.; Simonetti, E.; Appetecchi, G. B.; Carewska, M.; Montanino, M.; Kim, G. T.; Loeffler, N.; Passerini, S. Ionic Liquid Electrolytes for Safer Lithium Batteries: I. Investigation around Optimal Formulation. *J. Electrochem. Soc.* **2017**, *164*, A6026–A6031.
35. Simonetti, E.; Carewska, M.; Maresca, G.; De Francesco, M.; Appetecchi, G. B. Highly Conductive, Ionic Liquid-Based Polymer Electrolytes. *J. Electrochem. Soc.* **2017**, *164*, A6213–A6219.

DOI: 10.31635/ccschem.021.202101257
Citation: *CCS Chem.* **2021**, 3, 2762–2770
Citation denotes calendar and volume year of first online publication.
Issue Assignment: Volume 3 (2021), Issue 12

36. Liang, S.; Choi, U. H.; Liu, W.; Runt, J.; Colby, R. H. Synthesis and Lithium Ion Conduction of Polysiloxane Single-Ion Conductors Containing Novel Weak-Binding Borates. *Chem. Mater.* **2012**, *24*, 2316–2323.
37. Rohan, R.; Pareek, K.; Cai, W.; Zhang, Y.; Xu, G.; Chen, Z.; Gao, Z.; Dan, Z.; Cheng, H. Melamine–Terephthalaldehyde–Lithium Complex: A Porous Organic Network Based Single Ion Electrolyte for Lithium Ion Batteries. *J. Mater. Chem. A* **2015**, *3*, 5132–5139.
38. Kumar, Y.; Hashmi, S. A.; Pandey, G. P. Lithium Ion Transport and Ion–Polymer Interaction in PEO Based Polymer Electrolyte Plasticized with Ionic Liquid. *Solid State Ion.* **2011**, *201*, 73–80.
39. Boschin, A.; Johansson, P. Plasticization of NaX-PEO Solid Polymer Electrolytes by Pyr13X Ionic Liquids. *Electrochim. Acta* **2016**, *211*, 1006–1015.
40. Kamaya, N.; Homma, K.; Yamakawa, Y.; Hirayama, M.; Kanno, R.; Yonemura, M.; Kamiyama, T.; Kato, Y.; Hama, S.; Kawamoto, K.; Mitsui, A. A Lithium Superionic Conductor. *Nat. Mater.* **2011**, *10*, 682.
41. Dose, W. M.; Kim, S.; Liu, Q.; Trask, S. E.; Dunlop, A. R.; Ren, Y.; Zhang, Z.; Fister, T. T.; Johnson, C. S. Dual Functionality of Over-Lithiated NMC for High Energy Silicon-Based Lithium-Ion Batteries. *J. Mater. Chem. A* **2021**, *9*, 12818–12829.
42. Evans, T.; Olson, J.; Bhat, V.; Lee, S.-H. Effect of Organic Solvent Addition to $PYR_{13}FSI$ + LiFSI Electrolytes on Aluminum Oxidation and Rate Performance of $Li(Ni_{1/3}Mn_{1/3}Co_{1/3})O_2$ Cathodes. *J. Power Sources* **2014**, *265*, 132–139.
43. Usubelli, C.; Besli, M. M.; Kuppan, S.; Jiang, N.; Metzger, M.; Dinia, A.; Christensen, J.; Gorlin, Y. Understanding the Overlithiation Properties of $LiNi_{0.6}Mn_{0.2}Co_{0.2}O_2$ Using Electrochemistry and Depth-Resolved X-Ray Absorption Spectroscopy. *J. Electrochem. Soc.* **2020**, *167*, 080514.

DOI: 10.31635/ccschem.021.202101257
Citation: *CCS Chem.* **2021**, 3, 2762–2770
Citation denotes calendar and volume year of first online publication.
Issue Assignment: Volume 3 (2021), Issue 12